XII International Conference on Computational Plasticity. Fundamentals and Applications
COMPLAS XII
E. Oñate, D.R.J. Owen, D. Peric and B. Suárez (Eds)

MODELLING OF MATERIAL CUTTING WITH A MATERIAL MICROSTRUCTURE-LEVEL (MML) MODEL

Daniel NELIAS, Yancheng ZHANG, Tarek MABROUKI

Université de Lyon, CNRS, INSA-Lyon, LaMCoS, UMR5259, F69621, France,

email: Nelias.Daniel@insa-lyon.fr, lamcos.insa-lyon.fr
email: Tarek.Mabrouki@insa-lyon.fr, lamcos.insa-lyon.fr

Key words: Material microstructure-level cutting model, Crystal plasticity, Johnson-Cook law behaviour.

Abstract. In this research work a material microstructure-level cutting model (MML cutting model) is presented. The crystal plasticity theory is adopted for modeling the cutting of the titanium alloy Ti–6Al–4V in orthogonal case. In this model, the grains of the studied material are explicitly presented, and their orientation angles and slip system strength anisotropy are considered as the main source of the microstructure heterogeneity in the cutting material. To obtain the material degradation process, the continuum self-consistent intra-granular damage model and discrete cohesive zone inter-granular damage model, were developed, wherein the zero thickness cohesive element is implemented to simulate the bond between grain interfaces. This model was validated by a comparison with compression tests from literature. Results demonstrate the possibility to capture the influence of the microstructure on the material removal in terms of chip formation. Particularly, it is demonstrated that the grain orientation angle plays an important role for the chip segmentation and its periodicity during the cutting process.

1 INTRODUCTION

Metal cutting is one of the most widespread processes, in which one or many edges perform material removal in order to respect some criteria of qualification required to the final workpiece specifications (geometrical dimensions, surface finish, etc.). Despite the advances underlined in the development in the field of machine-tools, the monitoring and the process controlling, the optimization of cutting process is not yet overcame. This is due to the complexity of the multi-physic phenomena underlying the tool-workpiece interaction.

In industries most cutting operations are still mainly based on preliminary tests generally dictated by experimental models. The coefficients of these models are obtained with experimental tests codified by the scientific community and the industrial sector concerned. Methods of measurement are standardized to allow their transmission and their interchangeability. Analytical orthogonal models of two dimensional representation of cutting are usually adopted for these experimental scientific approaches [1], [2]. This has helped to develop empirical models derived from the well-known couple workpiece-tool (CWT)

methodology [3]. Thus, values characterizing the cutting operation (power consumption, specific energy, cutting force, chip thickness, etc.) are associated to operating conditions and qualified with more or less rigor.

Moreover, due to the complexity of the phenomena met during cutting, the small size of the tool-workpiece interaction area, the strong temperature gradients occurring, etc. the numerical methodology is becoming a helpful method in the current activities concerning the elaboration of machining models. This way, among others, benefits essentially from the efficiency of numerical adopted methods such as the finite element method (FEM). In general, it is noted that the current numerical simulations give more specific and refined results about the distribution of strain field, stress and/or temperature within the material being machined and the tool, etc. In this framework, Lin et al. [4] have elaborated a *2D* cutting model and adopted a line separation criterion for modeling the chip detachment. Baker et al. [5] adopted a remeshing technique with an implicit scheme to ensure convergence by avoiding high mesh distortion. Mabrouki et al. [6] introduced the fracture energy method to capture material degradation process and simulate chip genesis. Moreover, to analyze the chip formation and shear localisation for machining titanium alloys, Calamaz et al. [7] introduced a strain softening effect to the strain, strain rate, and temperature dependent flow stress laws.

However, the pertinence of such classical cutting models is greatly depending on the accuracy of input parameters and the scale of the model adopted. To understand more accurately what happens locally at the tool-workpiece interface, various micro-scale models have been proposed in the literature. Wherein, some researchers [8], [9] have studied the effect of the mechanism of material strengthening on the specific cutting energy variation when considering the micro-cutting level.

The study of tool-workpiece interaction can be carried out based on multi-scale approaches. In this framework, despite that there is no consensus among the scientific community on the definition of cutting scale. The global point of view consider that macroscopic approach deals with the overall behavior of the cutting system dynamics to predict for example the vibration effect on the workpiece behaviour (chatter, etc. Other cutting studies concern a more fine size named mesoscopic scale where aspects linked to chip formation such as its segmentation are pointed out. Other approaches, consider a more refine scale named microscopic scale in which material microstructure and phase transformations are studied by highlighting the induced results from the machining operation. It is important to note that the transition from one scale to another constitutes usually actual difficulties regarding the consideration of the whole machining system and its interactions. One of the first micro cutting models that considered the effect of the material microstructure is that published in [10][11][12].

In order to capture material microstructure effect during cutting operation, the crystal plasticity presents an interesting direction that can help to bring more physical comprehension. In this framework, the present contribution focuses to show the methodology that help to build a material microstructure cutting model based on the exploitation of both crystal plasticity and bonding relationship between grains via the consideration of cohesive

elements. The application to the orthogonal cutting of titanium alloy Ti–6Al–4V is illustrated in this paper.

2 TITANIUM ALLOY TI-6AL-4V MICROSTUCTURE AND ITS CUTTING

Titanium alloy Ti-6Al-4V has received considerable interest with wide range of applications in aerospace, automotive, chemical, and medical industries. However, this specific material generates segmented chip even at very low cutting speed, which may affect the machined surface integrity and introduce chatter instability of the machining process.

Many phenomenological cutting models have adopted various numerical methodologies, numerical software and different behavior laws to simulate the chip formation [5], [6], [7]. Among them, some the authors have presented results when cutting with high cutting speeds (sometimes more than 200 m/min) which is far from what is recommended by typical industrial applications for machining titanium alloy Ti–6Al–4V (30 ~ 70 m/min for a long term machining). However, in experimental observations on the chip for cutting speeds (30 ~ 90) m / min [13] it was noted that the segments of the chip have some aperiodic forms. This is presented by smaller randomly distributed segments among the continuous ones. So, the influence of microstructure, particularly the initial angle of orientation of the grains have to be taken into account both to explain refinery the chip formation and also to provide a physical understanding of the evolution of the machined surface integrity.

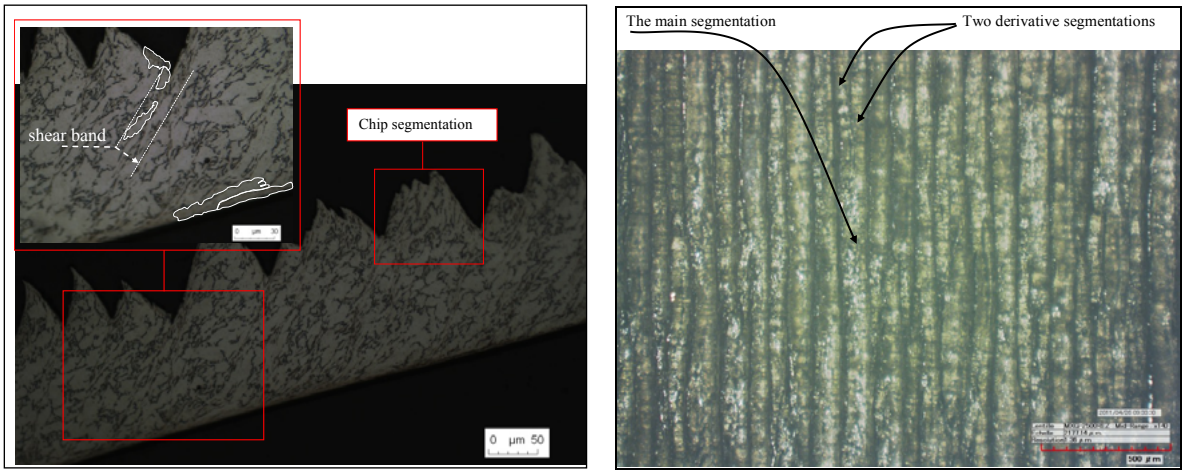

a) Lateral observation of the chip b) Spatial disposition of chip segments

Figure 1: Chip morphology during the cutting of Ti6Al4V (VC = 90 m/min, f = 0.1 mm/rev.)

The Titanium alloy Ti–6Al–4V has a duplex microstructure. It is composed, at room temperature, by the two phases α (hexagonal close-packed (HCP) crystal structure) and β (body center cubic (BCC) crystal structure). The Ti-6Al-4V offers an excellent balance of mechanical properties and density. In order to simplify the description of the material microstructure, which is relatively complex, only the primary phase α is considered for the

present study. In general case, metals with hexagonal structure (α phase) present four different crystallographic slip systems (CSS) as it is indicated in table and illustrated in Figure 2.

Table 1: Crystallographic slip systems (CSS) in metals with hexagonal structure

Name of (CSS)	Index of CSS	Slipping direction		Number of direction
Basal	(0001)	$[11\bar{2}0]$	$\vec{a}$	3
Prismatic	$(10\bar{1}0)$	$[11\bar{2}0]$	$\vec{a}$	3
Pyramidal of the 1st type	$(10\bar{1}1)$	$[11\bar{2}0]$	$\vec{a}$	6
Pyramidal of the 2nd type	$(10\bar{1}1)$	$[11\bar{2}3]$	$\vec{a}+\vec{c}$	12

The first three modes of slip (basal, prismatic and pyramidal of the 1st type) have the same sliding direction $[11\bar{2}0]$ continuing in the plan base. Only pyramidal slip systems have a sliding direction out of the plan base $[11\bar{2}3]$. This then allows the possibility of material deformation in the three directions of space. According to the literature the plans that have easier sliding are the basal and prismatic planes.

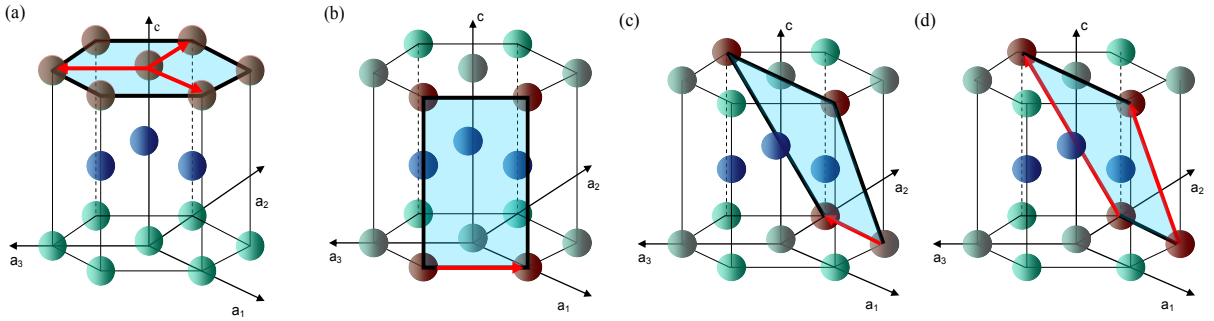

Figure 2: Slip geometries for the primary α-phase

Each grain in the polycrystal can be oriented by three angles according to the notation of Bunge (φ_1, Φ, φ_2) which corresponds to Euler angles: $\varphi_1 = \psi$ (precession), $\Phi = \theta$ (nutation) and $\varphi_2 = \varphi$ (intrinsic rotation) [14]. These angles define the relationship between the local crystal coordinate system (the orthogonal system [100]-[010]-[001], X′, Y′, Z′) of each grain with respect to a fixed specimen coordinate system (e.g. FE model in global coordinate system, X, Y, Z). A polycrystal aggregate is constructed by implementing the different Euler angles for each grain through the user subroutine (VUMAT) implemented within the explicit FE code ABAQUS.

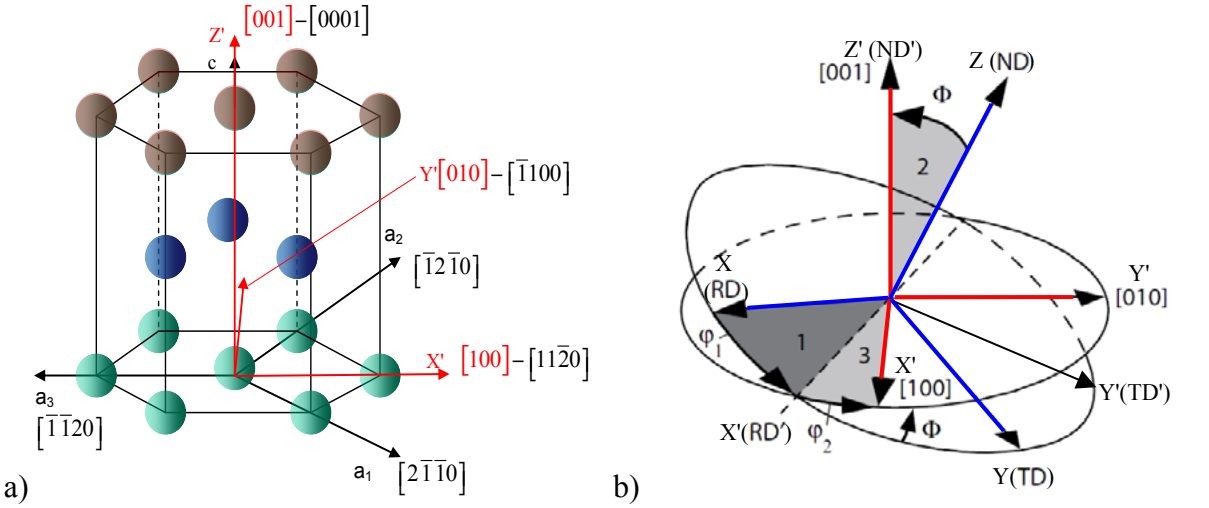

Figure 3: Slip geometries for the primary α-phase, a) Coordinate relationship between the Cartesian system and the Miller-Bravais system , (b) Rotation through the Euler angles φ_1, Φ, φ_2, in order 1, 2, 3.

The transformation matrix ***G*** **(**orthogonal transformation) for an individual grain from the local to the global coordinate systems is given by:

$$G = \begin{pmatrix} \cos\varphi_1\cos\varphi_2 - \sin\varphi_1\sin\varphi_2\cos\Phi & \sin\varphi_1\cos\varphi_2 + \cos\varphi_1\sin\varphi_2\cos\Phi & \sin\varphi_2\cos\Phi \\ -\cos\varphi_1\sin\varphi_2 - \sin\varphi_1\cos\varphi_2\cos\Phi & -\sin\varphi_1\sin\varphi_2 + \cos\varphi_1\cos\varphi_2\cos\Phi & \cos\varphi_2\cos\Phi \\ \sin\varphi_1\sin\Phi & -\cos\varphi_1\sin\Phi & \cos\Phi \end{pmatrix} \quad (1)$$

According to [14] the texture of Titanium alloy Ti-6Al-4V is mainly dependent on the Φ angle. Therefore in what follows the variation of the other two Euler angles will not be considered.

3 CONSTITUTIVE LAWS IN CRISTAL PLASTICITY AND APPROACHES OF MICRO-TO-MACRO PASSAGE

In this section a cutting model based on material microstructure-level (MML) is presented to simulate the machining operation of heterogeneous materials. Although the model is applied for the simulation of ductile titanium alloy Ti-6Al-4V, the proposed algorithm is general enough to be used for many other crystalline structure materials. Following the work of Chuzhoy et al. [10], the model consists of three main procedures that are integrated into the elaborated FE cutting model.

- The adoption of a polycrystal strategy model.
- The consideration of material flow law as intra-granular and inter-granular coupled damage models.
- The generation of the geometrical model considering the material microstructure (presence of hexagonal grain shape).

3.4 Intra-granular behavior

To develop a cutting model based on the material microstructure, three levels can be considered: The first one concerns the material behavior at the crystallographic scale (micro). The second one deals with the material behavior at the grain level (meso). The third one deals with the overall material behavior (macro)

Figure 4 shows, for a time increment, the scale transition between the three previous levels. The stresses and strains in the slip system are calculated on a micro scale and mean tensor stress and strain are expressed on a macroscopic scale. It is important to mention that the calculation is performed by considering in the modeling the various activated slip systems for different orientations within a representative elementary volume (REV). The latter is the smallest volume for which a local average behavior is identifiable and transferable to a higher volume in homogeneous conditions. For a polycrystal, a volume that includes a sufficient number of grains is considered to represent the material characteristics.

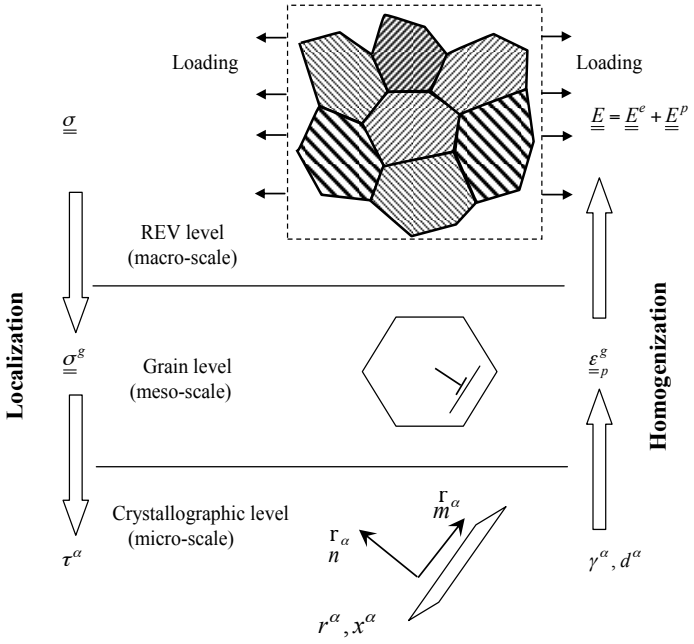

Figure 4: Schematic representation of the micro-macro polycrystal model. The constitutive law is written on slip systems of each grain

The polycrystal formulation of Cailletaud [15] was adopted. The localization rule of Kröner [16] which allows the passage from macro scale to the average stress in each grain is also adopted (Eq. (2)) The stress is corrected and is valid for a polycrystal with an identical nature grain and a macroscopically isotropic elasticity.

$$\underline{\underline{\sigma}}^g = \underline{\underline{\sigma}} + \alpha_T \underline{\underline{\underline{\underline{C}}}} : \left(\underline{\underline{E}}^{\mathrm{p}} - \underline{\underline{\varepsilon}}_p^g \right) \tag{2}$$

where:

$$\underline{\underline{\sigma}} = \sum_g c_g \underline{\underline{\sigma}}^g, \qquad \underline{\underline{E}}^p = \sum_g c_g \underline{\underline{\varepsilon}}_p^g \tag{3}$$

- $(\underline{\underline{\sigma}}, \underline{\underline{\sigma}}^g)$ et $(\underline{\underline{E}}^p, \underline{\underline{\varepsilon}}_g^p)$ are mean and in grain stress and plastic deformation tensors, respectively.

- α_T is the Taylor coefficient

- $\underline{\underline{\underline{\underline{C}}}}$ is the elastic tensor

- c_g is the concentration of each orientation considered in a grain.

The passage at the slip system is based on the critical resolved shear stress (Eq. (4)). On each slip system, Schmid's law led to a yield criterion Eq. (5)). The slip rate $\dot{\gamma}^s$ (sum, in a grain, of all slips in the same direction) corresponding to a slip system, s, is given by a viscoplastic constitutive law (Eq. (6)).

$$\tau^s = \underline{\underline{\sigma}}^g : \underline{\underline{\mu}}^s = \frac{1}{2}\underline{\underline{\sigma}}^g : (\vec{n}^s \otimes \vec{m}^s + \vec{m}^s \otimes \vec{n}^s) \tag{4}$$

$$f_s = \left|\tau^s - x^s\right| - r^s - k^s < 0 \tag{5}$$

$$\dot{\gamma}^s = \left\langle \frac{f_s}{K} \right\rangle^n \text{sign}(\tau^s - x^s), \quad \text{avec} \left\langle x \right\rangle = Max(x,0) \tag{6}$$

where τ^s the resolved shear stress characterized by a slip plane with a direction $\vec{m}^s$ and a normal $\vec{n}^s$. $\underline{\underline{\mu}}^s$ is the Schmid's tensor (said also the orientation tensor), k is the yield stress.

According to the sign of slip direction, the critical resolved shear stress τ^s is introduced through an additive hardening via the variables x^s and r^s. A slip system will be activated when $\tau^\alpha > (x^\alpha + r^\alpha)$ or $\tau^\alpha < (x^\alpha - r^\alpha)$. The scalar variable r^α describes the isotropic hardening beyond the yield flow by dislocations accumulated statistically (Eq.(7)). The law of this scalar considers interactions between slip systems via the components of h_{sr} of the interaction matrix. The latter is constructed by referring to material crystallographic data and knowledge of the slip physics. The scalar variable x^α describes kinematic hardening associated with each slip system and characterizes the position of the center of the material flow surface. Physically it indicates the presence or development of intra-granular inhomogeneities (precipitations, inclusion, etc.). Its law of evolution is given by Eq. (8).

$$r^s = R_0 + Q\sum_r h_{sr}\left(1 - e^{-b\gamma^r}\right)\left(1 - \left(\frac{T - T_0}{T_f - T_0}\right)^m\right) \tag{7}$$

$$\dot{x}^s = \left(C^s - d^s\, x^s\right)\dot{\gamma}^s \tag{8}$$

where C^s, d^s, R_0, Q, b, n, m, T_0, and T_f are data dependent parameters for the considered slip system.

By integration over an increment of time, it is possible to retrieve γ^s and determine the average plastic deformation at the grain (Eq. (9)). The average plastic deformation is determined by the second term of Eq.(3).

$$\underline{\underline{\varepsilon}}_p^g = \sum_{s \in g} \gamma^s \underline{\underline{\mu}}^s \tag{9}$$

The proposed approach is guided here by the physical mechanisms of dislocations in the crystal lattice. Nevertheless, the model can also be qualified as macroscopic. Averaging the plastic deformation on a polycristal grains corresponds to a global approach compared to which is localized in the grains.

In addition, to describe the intergranular damage associated with the previous approach, the model of Lemaître and Chaboche was adopted [17].

3.5 Inter-granular behavior

To simulate the inter-granular behavior, a traction-separation cohesive model (Fig. 8.47) has been programmed in a user routine VUMAT. Cohesive elements have been defined at grain boundaries.

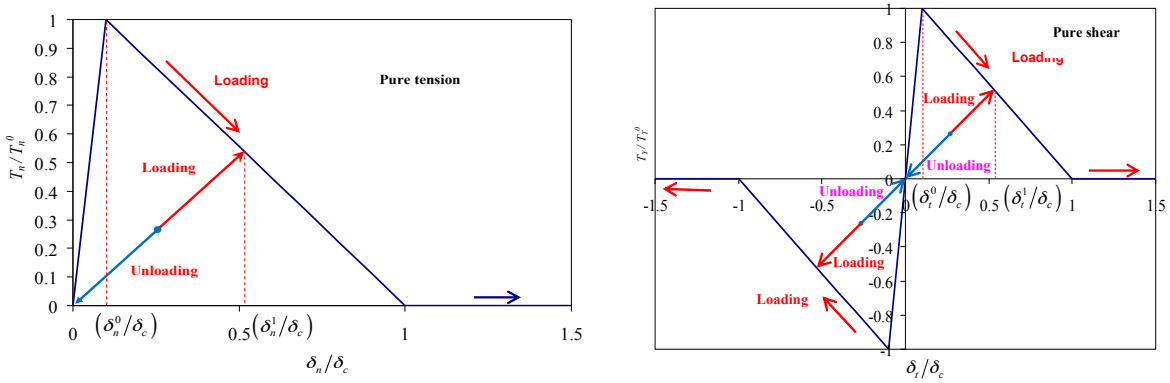

Figure 5: Response to the constitutive law traction-separation, a) Pure tension (b) Pure shear

In the adopted cohesive law the normal tension T_n and the tangential shear T_t at the grain interface are linear with the normal δ_n and tangential δ_t displacements, respectively. In the local coordinate system of a finite element, the stress-strain relationships are defined by according to the Eq. (10).

$$\begin{cases} T_n = k_n \delta_n = \dfrac{\delta_n^0}{\delta_n^1} k_n^0 \left(1 - D_n\right) \delta_n \\ T_t = k_t \, \delta_t = \left|\dfrac{\delta_t^0}{\delta_t^1}\right| k_t^0 \left(1 - D_t\right)\left(1 - D_n\right) \delta_t \end{cases} \tag{10}$$

The parameters k_n and k_t are the stiffness of the cohesive zone in the normal and tangential directions to the interface of two adjacent grains. Parameters (k_n^0, k_t^0) and (δ_n^0, δ_t^0) are the initial stiffness and displacement (corresponding to the initiation of damage), respectively. The parameters D_n and D_t are maximum values of damage describing the process of grain interface debonding. The damage is assumed to be initiated when the maximal stress ratio given by Eq. (11), reaches the value of one.

$$max\left\{\frac{\langle T_n \rangle}{T_n^0\left(1 - D_n\right)}, \frac{\left|T_t\right|}{T_t^0\left(1 - D_t\right)\left(1 - D_n\right)}\right\} = 1 \tag{11}$$

Where T_n^0 and T_t^0 are maximum normal tensile and tangential shear stresses (corresponding to the fracture modes *I* and *II*), respectively. After the damage initiation, the constitutive equations of the cohesive elements at grains interfaces reflect irreversible traction-displacement relationships (Eqs. (12) and (13)) [18].

$$\begin{cases} T_n = T_n^0 (1 - D_n), \quad D_n = \dfrac{\delta_n - \delta_n^0}{\delta_c - \delta_n^0} \quad (\text{loading}) \\ T_n = T_n^0 (1 - D_n) \dfrac{\delta_n}{\delta_n^1}, \quad D_n = \dfrac{\delta_n^1 - \delta_n^0}{\delta_c - \delta_n^0} \quad (\text{unloading}) \end{cases} \tag{12}$$

$$\begin{cases} T_t = T_t^0 (1 - D_t)(1 - D_n) sign(\delta_t), \quad D_t = \dfrac{\left|\delta_t\right| - \delta_t^0}{\delta_c - \delta_t^0} \quad (\text{loading}) \\ T_t = T_t^0 (1 - D_t)(1 - D_n) \dfrac{\delta_t}{\left|\delta_t^1\right|}, \quad D_t = \dfrac{\left|\delta_t^1\right| - \delta_t^0}{\delta_c - \delta_t^0} \quad (\text{unloading}) \end{cases} \tag{13}$$

where δ_c the critical distance regarding traction (for the grain interface debonding).

4 MATERIAL MICROSTRUCTURE-LEVEL (MML) CUTTING MODEL AND SOME RESULTS

Before developing the cutting model, a compression numerical test was carried out based on the polycristal methodology. The number of grains (137 grains), their dimensions and orientations were similar to those set by Mayeur [19] in a fatigue study on titanium alloys.

The grains have a geometrical aspect defined by the values $\left(l/h\right) = 1,67$ ($l = 30\ \mu m$). This compression model was calibrated to the model published in [20] (Figure 6). Results for temperatures of 300 and 500 °C and a strain rate of 2000 s^{-1} are in agreement with those of Lee et al. [20]. Thus, this model shows an interesting prediction regarding the material behavior on a macro scale and considering material micro properties.

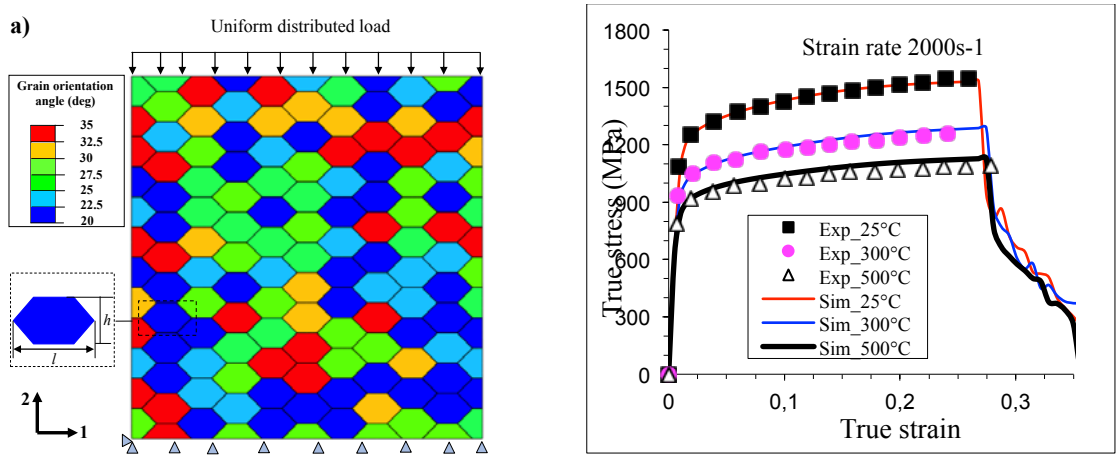

Figure 6: Numerical compression test a) Grain initial distribution b) comparison with [20]

The developed microstructural cutting model for titanium alloy (Ti-6Al-4V) is based on crystal plasticity to enhance the understanding of the tool-material interaction. This aim is to assess the importance of the grain orientation on the genesis of the chip. The geometrical model adopted is shown in Figure 7. It is characterized by a regular distribution of grain initial orientation 0°, 30°, 45° and 60°.

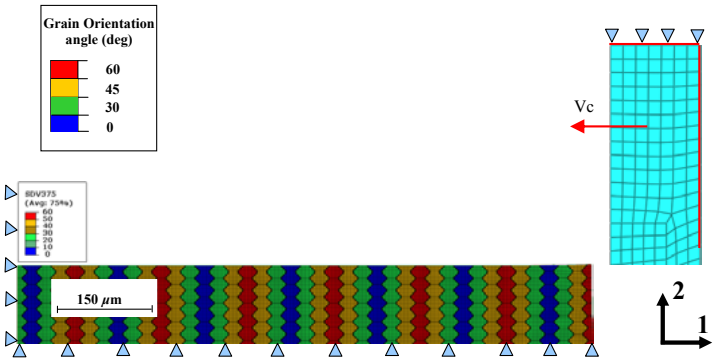

Figure 7: Geometric cutting model based on the crystal plasticity with a regular distribution of grain orientations

The corresponding results (Figure 8) shows (for $V_C = 90\ m/min$ and $f = 0.1\ mm/rev$), the spatial distribution of grains after the chip formation. They are identified by their initial orientations. While the overall morphology in its details is not really similar to the chip obtained experimentally in (Figure 1.a), however, it can be underlined that the valley area of the segmented chip is located in the highest grain initial orientation. In contrary, the chip peak is characterized by the presence of a lower initial grain orientation. Also, it can be observed

periodically a primary shear band, characterized by a significant equivalent deformation. These bands correspond to grains whose initial orientation is the largest (Figure 8.a). Therefore, for a random distribution of initial grain orientations, (which correspond to the physical reality), it can be expected to obtain aperiodic chip segments. This explains, among others, the appearance of small segments interspersed from time to time between two consecutive segments clearly formed on the chip.

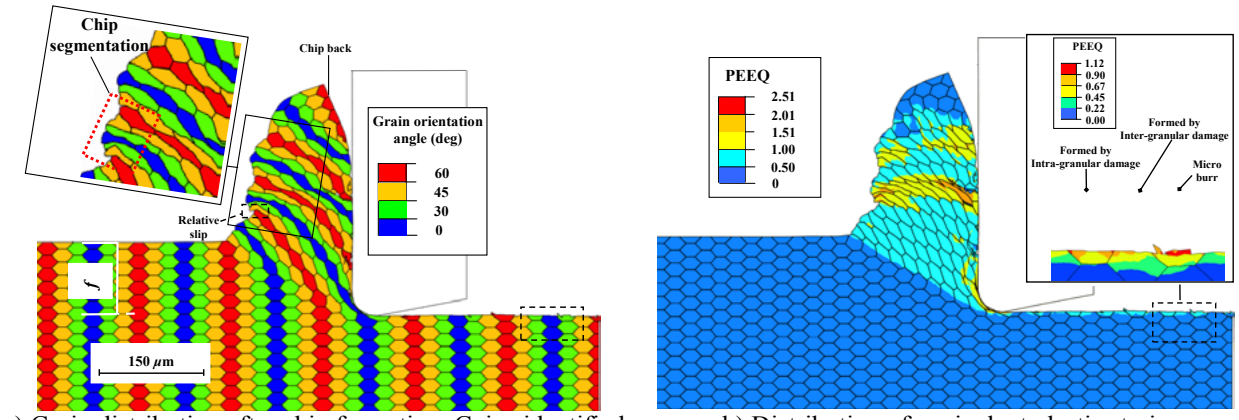

a) Grain distribution after chip formation. Gains identified by their initial orientations

b) Distribution of equivalent plastic strain

Figure 8: Microstructure cutting model results for (V_C = *90 m/min, f = 0.1 mm/rev*)

In addition, some areas of plastic deformation can be noticed on the cut surface and at the interface of a few grains (Figure 8.b). This model shows that the higher the cutting speed, the higher the cut surface has geometric imperfections and large areas of plastic deformation (Figure 9). It is also observed that these defects are more pronounced for large values of feed rates (Figure 10).

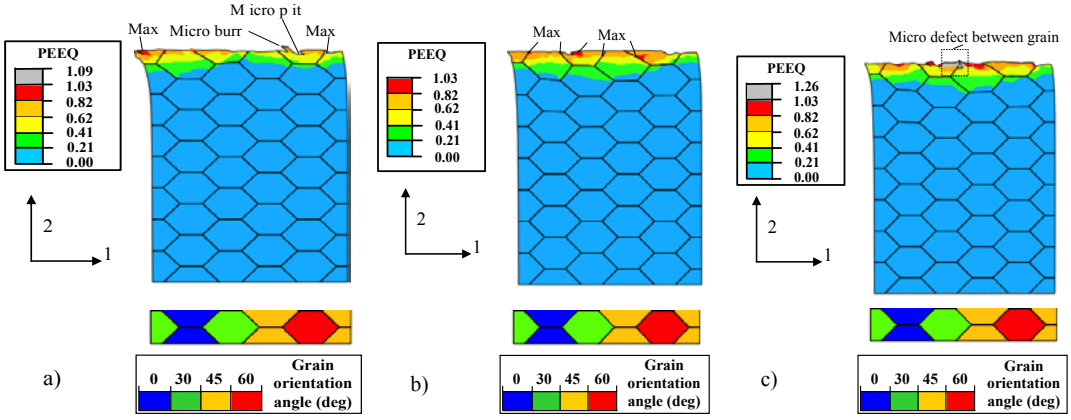

Figure 9: Distribution of equivalent plastic strain for *f = 0.1* mm/rev a) V_C = 30 m/min, b) V_C = 60 m/min, c) V_C = 120 m/min

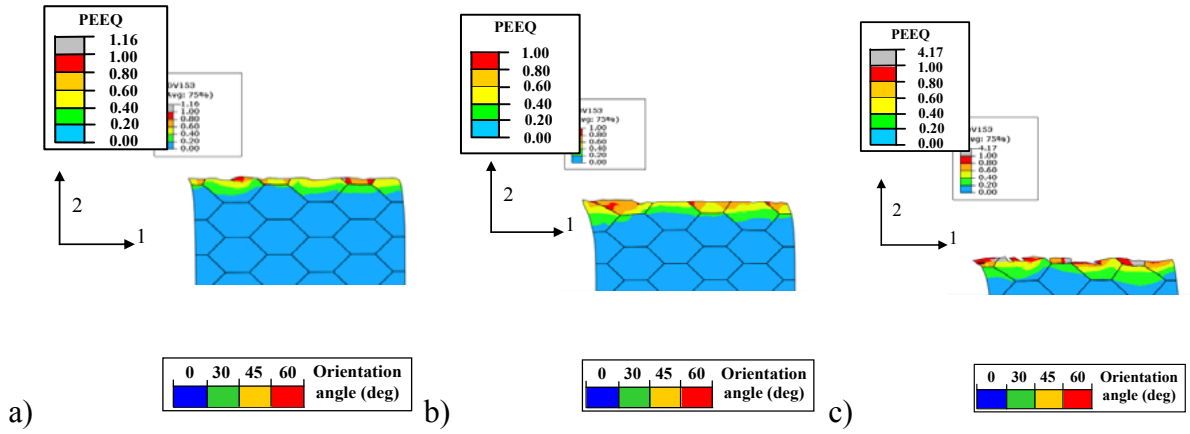

Figure 10: Distribution of equivalent plastic strain for $V_C = 60$ *m/min*, a) $f = 0.06$ mm/rev, b) $f = 0.1$ *mm/rev*, c) $f = 0.15$ *mm/rev*

5 CONCLUSION

A material microstructure level (MML) cutting model based on crystal plasticity is proposed for Titanium alloy Ti–6Al–4V. To model the material degradation process yielding to chip formation, both intra-granular (based on crystallographic slip in the grains) and inter-granular (formalized by zero thickness discrete cohesive elements) damage models have been developed and implemented with user subroutines in the FE commercial package Abaqus/Explicit. Based on the developed MML cutting model, it is shown that:

- The chip formation mechanism is well described by shear slip between grains and by crystallographic slip within the grains.

- It can be also observed that intra-granular damage is at the origin of micro-burrs visible on the newly formed surface, whereas inter-granular damage produces smoother cut surface.

- According to the variation of cutting conditions on chip formation, it was shown that the higher is the cutting speed, more pronounced are both the segmented chip and micro-defects at its back.

- It is also found that the surface roughness is likely to increase, as well as the maximum plastic strain, when increasing the feed rate whereas the effect of the cutting speed seems to be less.

This proposed cutting model has the capacity to simulate the material removal process while considering some features of the microstructure. However, it should be seen as a first step toward a more sophisticated approach. Note that this approach does not require anymore the description a priori of the cutting path, usually by cohesive elements, that is to say the tool trajectory within the workpiece is free which also open new possibilities.

REFERENCES

[1] Merchant, M.E. *Mechanics of Metal Cutting Process*. J. Appl. Phys. (1945), 16:267–275.

[2] Oxley, P.L.B. *The Mechanics of Machining: An Analytical Approach to Assessing Machinability*, E. Horwood, Chichester, England, 1989.

[3] Standard: NF E66-520-1. *Domaine de fonctionnement des outils coupants - Couple outil-matière - Partie 1 : présentation générale.* 1997.

[4] Lin, Z.C. and Lo S.P. *A study of the tool-chip interface contact problem under low cutting velocity with an elastic cutting tool*. J. of Mat. Proc. Techn. (1997)7, 0 (1-3), 34-46.

[5] Bäker, M., Rösler, J., Siemers, C., 2002. A finite element model of high speed metal cutting with adiabatic shearing. Comput. Struct 80, 495–513.

[6] Mabrouki, T., Girardin, F., Asad, M., Rigal, J.F., 2008. Numerical and experimental study of dry cutting for an aeronautic aluminium alloy (A2024-T351). International

[7] Calamaz, M., Coupard, D., Girot, F., 2008. A new material model for 2D numerical simulation of serrated chip formation when machining titanium alloy Ti–6Al–4V. International Journal of Machine Tools & Manufacture 48, 275-288.

[8] Liu, K. and Melkote, S.N., 2006. Material strengthening mechanisms and their contribution to size effect in micro-cutting. Journal of Manufacturing Science and Engineering 128(3), 730–738.

[9] Asad, M., Mabrouki, T., Girardin, F., Zhang, Y., Rigal, J.F., 2011. Towards a physical comprehension of material strengthening factors during macro to micro-scale milling. MECHANIKA 17(1), 97-104.

[10] Chuzhoy, L., DeVor, R.E., Kapoor, S.G., Bammann, D.J., 2002. Microstructure-level Modeling of Ductile Iron Machining. ASME Journal of Manufacturing Science and Engineering 124, 162–169.

[11] Chuzhoy, L., DeVor, R.E., Kapoor, S.G., Beaudoin, A.J., Bammann, D.J., 2003. Machining simulation of ductile iron and its constituents, part 1: Estimation of material model parameters and their validation. Journal of Manufacturing Science and Engineering 125(2), 181–191.

[12] Chuzhoy, L., DeVor, R.E., Kapoor, S.G., 2003. Machining simulation of ductile iron and its constituents, part 2: Numerical simulation and experimental validation of machining. Journal of Manufacturing Science and Engineering 125(2), 192–201.

[13] Zhang Y.C., 2011. Numerical simulation approaches and methodologies for multi-physic comprehensions of Titanium alloy (Ti–6Al–4V) cutting. PhD thesis, INSA Lyon.

[14] Mayeur, R.J., 2004. Three dimensional modeling of Titanium-Aluminum alloys with application to attachment fatigue. Thesis, Georgia Institute of Technology.

[15] G. Cailletaud, A micromechanical approach to inelastic behaviour of metals. Int. J. Plasticity, (1992), Vol. 8, p. 55-73.

[16] E. Kröner, On the plastic deformation of polycrystals. Acta Metall. (1961), Vol. 9, p. 156-165.

[17] Chaboche J-L, Lemaître J, Benallal A and Desmorat R, *Mécanique des matériaux solides*. 3ème édition, (2009), Dunod, Sciences Sup, ISBN : 978-2-10-051623-0, 577 pages.

[18] J.D. Clayton, *Dynamic Plasticity and Fracture in High Density Polycrystals: Constitutive Modeling and Numerical Simulation*. Journal of Mechanics and Physics of solids. (2005), Vol.53, p. 261-301.
[19] Mayeur, R.J., 2004. Three dimensional modeling of Titanium-Aluminum alloys with application to attachment fatigue. Thesis, Georgia Institute of Technology.
[20] W.S. Lee, C.F. Lin, *Plastic deformation and fracture behaviour of Ti–6Al–4V alloy loaded with high strain rate under various temperatures*. Materials Science and Engineering A. (1998), Vol. 241, p. 48-59.